3-8-2011

Atomistic Study of Electronic Structure of PbSe Nanowires

Abhijeet Paul
NCN, Purdue University

Gerhard Klimeck
NCN, Purdue University, gekco@purdue.edu

Paul, Abhijeet and Klimeck, Gerhard, "Atomistic Study of Electronic Structure of PbSe Nanowires" (2011). *Birck and NCN Publications.* Paper 731.
http://dx.doi.org/10.1063/1.3592577

Atomistic study of electronic structure of PbSe nanowires

Abhijeet Paul and Gerhard Klimeck

Citation: Appl. Phys. Lett. **98**, 212105 (2011); doi: 10.1063/1.3592577
View online: http://dx.doi.org/10.1063/1.3592577
View Table of Contents: http://aip.scitation.org/toc/apl/98/21
Published by the American Institute of Physics

Atomistic study of electronic structure of PbSe nanowires

Abhijeet Paul[a] and Gerhard Klimeck
School of Electrical and Computer Engineering, Network for Computational Nanotechnology, Purdue University, West Lafayette, Indiana 47907, USA

(Received 12 March 2011; accepted 28 April 2011; published online 23 May 2011)

Lead Selenide (PbSe) is an attractive 'IV-VI' semiconductor material to design optical sensors, lasers, and thermoelectric devices. Improved fabrication of PbSe nanowires (NWs) enables the utilization of low dimensional quantum effects. The effect of cross-section size (W) and channel orientation on the band structure of PbSe NWs is studied using an 18 band sp^3d^5 tight-binding theory. The band gap increases almost with the inverse of the W for all the orientations indicating weak symmetry dependence. [111] and [110] NWs show higher ballistic conductance for the conduction and valence band compared to [100] NWs due to the significant splitting of the projected L-valleys in [100] NWs. © *2011 American Institute of Physics*. [doi:10.1063/1.3592577]

Appealing PbSe bulk properties: Lead selenide (PbSe) is a narrow, direct band gap semiconductor material [$\sim Eg^{bulk}$ =0.16 eV at 4 K (Refs. 1 and 2)] with useful electrical, optical, and lattice properties.[3–5] It is used extensively in optical devices,[3,6] lasers,[7,8] and thermoelectric devices.[4,9,10] The large Bohr exciton radius of about 46 nm in PbSe makes it a suitable system to study quantum confinement effects on electrons and holes.[6,11–13] Recent progress in multiple exciton generation in PbSe with higher optical efficiency has renewed interest in the optical properties of PbSe.[5] Extremely low thermal conductivity of PbSe [~2 W/m K in bulk[10] to ~0.8 W/m K in nanowires (NWs) (Ref. 14)] also makes it a suitable thermoelectric material.[4,10] PbSe can become a preferable material over Lead Telluride due to the higher availability of selenium (Se) compared to tellurium.[15]

Nanostructures PbSe: One dimensional nanostructures of PbSe like NW and nanorods combine the interesting bulk material properties as well as the quantum confinement effects which can lead to better thermoelectric[10,14] and optical[3] devices. The analysis of the physical properties in PbSe NWs will require proper understanding of the electronic structure, which is the theme of the present letter.

PbSe NW growth technologies: With recent advances in the growth and process technology, the fabrication of PbSe NWs have become very efficient and controlled. PbSe NWs are developed using a variety of methods like, chemical vapor transport method,[9] oriented nanoparticle attachment,[11] electro-deposition without catalyst[12] and with catalyst,[16] hyper-branching,[17] growing PbSe structures on phosphate glass,[18] etc. These methods enable PbSe NWs fabrication with a variety of growth directions and surfaces.

PbSe crystal structure: Bulk PbSe has a stable rocksalt structure with a coordination number of six at room temperature (300 K) and normal atmospheric pressure.[1,15] The lattice constant is 0.6121 nm (Ref. 1) at T=4 K, which is also utilized in our band structure calculations. The PbSe NWs are constructed using the same bulk structure with three different wire axis orientations of [100], [110], and [111] (Fig. 1).

Electronic Structure calculation: The main methods for analyzing the lead salt structures are (1) continuum method like 4/8-band k×p,[6] (2) semi-empirical atomistic methods like tight-binding (TB),[2,19] pseudopotential approaches[20] or (3) first principles methods.[13,15,21,22] The 4/8-band k×p method captures some quantum confinement effects, however, it fails to capture the interaction of various valleys present along the *L-K* and *L-X* directions, the band anisotropy and the correct frequency dependent dielectric function.[13,19,20] The first principle calculations are highly accurate but the demand for computational power is very high and these methods are limited to solving only small structures with few thousand atoms.[19,23] The semi-empirical methods are versatile in terms of the involved physics and can handle a large number of atoms [≥10 million atoms (Ref. 23)] making them suitable for electronic structure and transport calculation in realistic device structures. However, an integral part of these methods is the requirement of correct semi-empirical parameter sets to properly represent the electronic structure properties like band gaps, effective masses, wave-function symmetry, etc. In this letter we utilize a semi-empirical atomistic TB method based on sp^3d^5 formulation with spin orbit coupling (SOC) optimized for bulk Pb salts by Lent *et al.*[2] to calculate the electronic structure in NWs. The inclusion of SOC is important in PbSe since both conduction band (CB) and valence band (VB) have strong p-contributions from Pb and Se atoms, respectively.[13,19]

Surface atoms: The TB parameters developed for bulk Pb salts (Ref. 2) are also applied to nanostructures with finite boundaries. The surface atoms are not passivated for Pb salt nanostructures. It has been previously shown that surfaces do not introduce states in the energy gaps of the bulk band

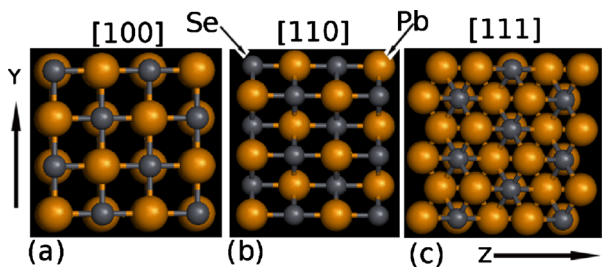

FIG. 1. (Color online) PbSe unit cell with wire axis orientations (x) along (a) [100], (b) [110], and (c) [111]. The W is of 2.5 nm(Y)×2.5. Lead (Pb) and selenium (Se) atoms are shown.

[a]Electronic mail: abhijeet.rama@gmail.com.

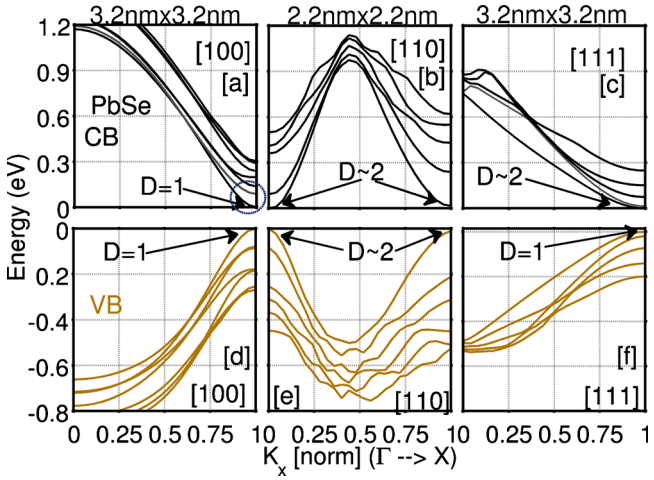

FIG. 2. (Color online) Band structure of PbSe NWs for (a) [100], (b) [110], and (c) [111] channels. The CBM and VBM are normalized to zero for simplified band comparison. Only the first 5–10 sub-bands are shown.

structure, even though they are not passivated[19] and the same is obtained in the present study. The surface states are mainly p-like for Pb salts which are strongly coupled with orbitals of atoms at the interior unlike the zinc-blende semiconductors where atoms are described by hybrid sp^3 orbitals which remain uncoupled at surfaces, forming dangling bonds.[24] The lack of surface passivation has also been pointed out by the first principle calculations in stoichiometric Pb salt nanostructures.[13,22]

Electronic Structure: The bulk effective masses calculated using the TB parametrization in Ref. 2 is obtained for (i) electrons as $m_e^{\parallel}/m_e^{\perp}=0.087(0.07)/0.036(0.04)=2.4(1.85)$ and (ii) holes as $m_h^{\parallel}/m_h^{\perp}=0.094(0.068)/0.031(0.34)=2.9(2.0)$. The values in the parenthesis are from Ref. 1. The TB parametrization in Ref. 2 (TB_A) is preferred over the parametrization in Ref. 19 (TB_B) since the TB_A model captures the mass anisotropy quite well, an important requirement for TB models as pointed in Ref. 20.

The band structure of CB and VB for PbSe NWs are shown in Fig. 2 for three different wire orientations. For all the wires the CB minima (CBM) and VB maxima (VBM) are normalized to zero to enable a better comparison of the valleys. Few important points to observe are (i) bulk L valleys are projected at the Brillioun zone edge at X for all orientations (Fig. 2). The [110] wire has an additional projected valley at the Γ position [Figs. 2(b) and 2(e)], (ii) [100] NW show a degeneracy (D) of 1 for both CB and VB due to strong valley splitting, however [110] and [111] NWs show a D of nearly 2 (extremely small valley splitting) for the positive 'k' states.

The CBM and VBM variation with cross-section size (W) and orientation are shown in Fig. 3(a). All the orientations show quite similar band-edge variation with W. As the cross-section size decreases the geometrical confinement increases which pushes the CBM (VBM) higher (lower) in energy. The variation in the bandedges with W also compare surprisingly well with a previous 4–band k.p. calculation done for [111] cylindrical PbSeNWs [Ref. 25]. Bandedge result obtained using TB also compare well with the k.p. result for 4nm diameter cylindrical PbSe nanowires [Ref. 26]. However, the band curvatures are very different in both the cases. These results are not shown here for the sake of brevity. The bandgap variation with W in PbSe NWs can be fitted to the following analytical express, :

$$Eg = \beta/(W)^{\alpha}, \tag{1}$$

where α represents the power law dependence on W.

For [111] NWs the value of $\beta,(\alpha)$ is 1.726 (0.8734). For [110] NWs these values are $[\beta,(\alpha)]$ 1.564 (0.8592) and for [100] NWs these values are $[\beta,(\alpha)]$ 1.87(1.072). The band gap values [Fig. 3(b)] roughly show an inverse relation with W for all the NW orientations which is very different from the prediction of effective mass approximation ($Eg \propto W^{-2}$). Similar results for Eg have been obtained by other independent calculations carried out in PbSe nanostructures using first principle calculations[13] as well as TB calculations.[19] This justifies the application of TB electronic structure calculation which correctly captures the quantum confinement effects in ultrascaled PbSe NWs.

Ballistic conductance: Transport properties of PbSe NWs are revealed by the electronic conductance which is calculated using Landauer's formula.[27] Figure 4 shows the normalized one-dimensional ballistic conductance for electrons in the PbSe NWs for 3 different orientations. [110] and

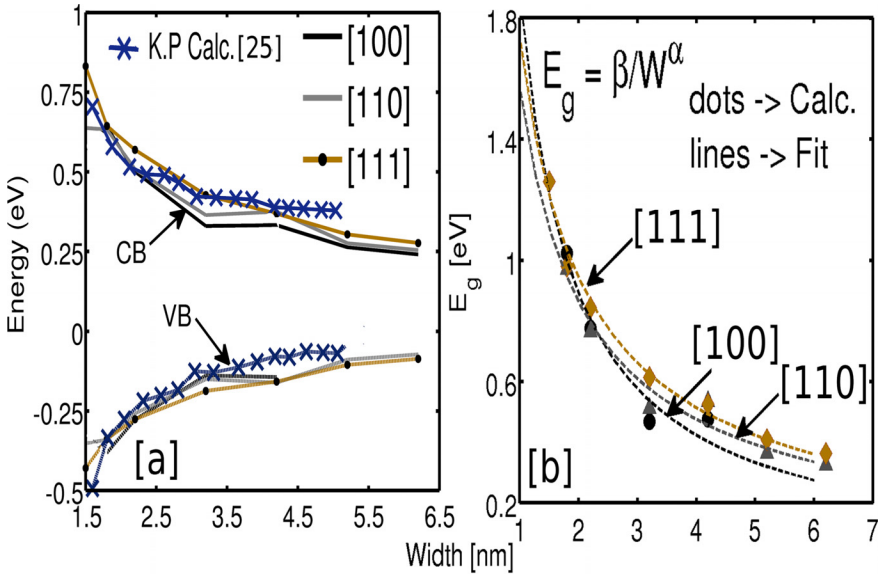

FIG. 3. (Color online) (a) Band edges for square PbSe NWs with [100], [110], and [111] channel orientations. Band edge result using four band k×p calculation for cylindrical PbSe NWs from Ref. 25. (b) Band gap variation for all the NWs. Dots are TB values and lines are analytical fits with W.

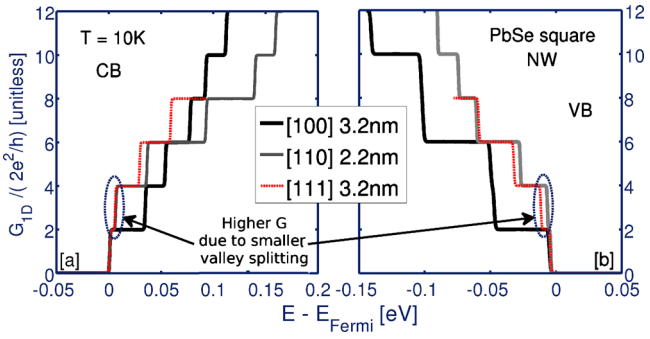

FIG. 4. (Color online) Ballistic conductance in PbSe NWs for (a) CB and (b) VB for three different wire orientations at T=10 K. The temperature comes from the Fermi-Dirac distribution of the carriers.

[111] oriented wires show higher G value for both the CB and the VB compared to [100] NWs. A larger valley splitting in the CB and the VB in [100] NWs decrease the conductance compared to the other two orientations. The normalized conductance increases in steps of 2 for [100] NWs for the CB but not for the VB (Fig. 4) which shows that the CB and the VB are not entirely symmetric in energy, a result similar to the one given in Ref. 20. Thus, transport characteristics show the influence of geometrical confinement and channel orientation.

Summary and Outlook: PbSe NWs have tremendous potential of becoming the next generation thermoelectric and optical devices. The proper understanding of the physical properties of these ultrascaled PbSe NWs will depend strongly on the correct electronic structure calculation. We have presented the application of semi-empirical tight-binding theory to these NWs to understand the variation in conduction and VBs and the position of the important energy valleys. The variation in the band gap and the band edges with NW cross-section size is strongly influenced by the W and channel orientation. Simple effective mass theory cannot predict the band gap variations. The valley splitting strongly depends on the type of geometrical confinement as reflected in the ballistic conductance of the PbSe NWs. [110] NWs provide the maximum ballistic conductance for both the CB and VB. The TB analysis of electronic structure opens door to explore the optical and thermoelectric effects in PbSe NWs.

Financial support from MSD under SRC, Nanoelectronics Research Initiative through MIND, NSF and Purdue University and computational support from nanoHUB.org, an NCN operated and NSF (Grant No. EEC-0228390) funded project are gratefully acknowledged.

[1]O. Madelung, U. Rssler, and M. Schulz, *Springer Materials*, The Landolt-Börnstein Database (Springer GmbH, Heidelberg, 2010).
[2]C. S. Lent, M. A. Bowen, J. D. Dow, R. S. Allgaier, O. F. Sankey, and E. S. Ho, Superlattices Microstruct. **2**, 491 (1986).
[3]J. Diezhandino, G. Vergara, G. Pérez, I. Génova, M. T. Rodrigo, F. J. Sánchez, M. C. Torquemada, V. Villamayor, J. Plaza, I. Catalán, R. Almazán, M. Verdú, P. Rodríguez, L. J. Gómez, and M. T. Montojo, Appl. Phys. Lett. **83**, 2751 (2003).
[4]I. Kudman, J. Mater. Sci. **7**, 1027 (1972).
[5]M. Ji, S. Park, S. T. Connor, T. Mokari, Y. Cui, and K. J. Gaffney, Nano Lett. **9**, 1217 (2009).
[6]I. Kang and F. W. Wise, J. Opt. Soc. Am. B **14**, 1632 (1997).
[7]J. Fürst, H. Pascher, T. Schwarzl, M. Böberl, G. Springholz, G. Bauer, and W. Heiss, Appl. Phys. Lett. **84**, 3268 (2004).
[8]M. Rahim, A. Khiar, F. Felder, M. Fill, and H. Zogg, Appl. Phys. Lett. **94**, 201112 (2009).
[9]M. Fardy, A. I. Hochbaum, J. Goldberger, M. M. Zhang, and P. Yang, Adv. Mater. (Weinheim, Ger.) **19**, 3047 (2007).
[10]W. Liang, O. Rabin, A. I. Hochboum, M. Fardy, M. Zhang, and P. Yang, Nano Res. **2**, 394 (2009).
[11]K. S. Cho, D. V. Talapin, W. Gaschler, and C. B. Murray, J. Am. Chem. Soc. **127**, 7140 (2005).
[12]J. E. Hujdic, D. K. Taggart, S.-C. Kung, and E. J. Menke, J. Phys. Chem. **1**, 1055 (2010).
[13]Y. Gai, H. Peng, and J. Li, J. Phys. Chem. C **113**, 21506 (2009).
[14]D. E. Gray, *American Inst. of Phys. Handbook.* 3rd ed. (McGraw-Hill, New York, 1972) p. 100.
[15]L. Zhang and D. J. Singh, Phys. Rev. B **80**, 075117 (2009).
[16]X. S. Peng, G. W. Meng, J. Zhang, X. F. Wang, C. Z. Wang, X. Liu, and L. D. Zhang, J. Mater. Res. **17**, 10 (2002).
[17]M. J. Bierman, Y. K. A. Lau, and S. Jin, ACS Nano **7**, 2907 (2007).
[18]A. Lipovskii, E. Kolobkova, V. Petrikov, I. Kang, A. Olkhovets, T. Krauss, M. Thomas, J. Silcox, F. Wise, Q. Shen, and S. Kycia, Appl. Phys. Lett. **71**, 3406 (1997).
[19]G. Allan and C. Delerue, Phys. Rev. B **70**, 245321 (2004).
[20]J. M. An, A. Franceschetti, S. V. Dudiy, and A. Zunger, Nano Lett. **6**, 2728 (2006).
[21]M. Lach-hab, D. A. Papaconstantopoulos, and M. J. Mehl, J. Phys. Chem. Solids **63**, 833 (2002).
[22]A. Franceschetti, Phys. Rev. B **78**, 075418 (2008).
[23]G. Klimeck, S. S. Ahmed, N. Kharche, M. Korkusinski, M. Usman, M. Prada, and T. Boykin, IEEE Trans. Electron Devices **54**, 2090 (2007).
[24]S. Lee, F. Oyafuso, P. von Allmen, and G. Klimeck, Phys. Rev. B **69**, 045316 (2004).
[25]S. V. Goupalov, arXiv:1012.2424v1 (unpublished); This reference provides the only data for band-edge variation with wire width using k.p. calculations http://arxiv.org/abs/1012.2424.
[26]A. C. Bartnik, Al. L. Efros, W.-K. Koh, C. B. Murray, and F. W. Wise, Phys. Rev. B **82**, 195313 (2010).
[27]R. Landauer, IBM J. Res. Dev. **1**, 223 (1957).